RESEARCH ARTICLE

Human Mutation

OFFICIAL JOURNAL
HGVS
HUMAN GENOME VARIATION SOCIETY
www.hgvs.org

Alu-Repeat–Induced Deletions Within the *NCF2* Gene Causing p67-*phox*–Deficient Chronic Granulomatous Disease (CGD)

Marcus Gentsch,[1†] Aneta Kaczmarczyk,[2†] Karin van Leeuwen,[3,13] Martin de Boer,[3,13] Magdalena Kaus-Drobek,[2,12] Marie-Claire Dagher,[4] Petra Kaiser,[5] Peter D. Arkwright,[6] Manfred Gahr,[1] Angela Rösen-Wolff,[1] Matthias Bochtler,[2,12] Elizabeth Secord,[7] Pamela Britto-Williams,[7] Gulam Mustafa Saifi,[8] Anne Maddalena,[8] Ghassan Dbaibo,[9,14] Jacinta Bustamante,[10,11] Jean-Laurent Casanova,[10,11] Dirk Roos,[3†] and Joachim Roesler,[1*†]

[1]Department of Pediatrics, University Hospital Carl Gustav Carus, Dresden, Germany; [2]Structural Biology Laboratory, International Institute of Molecular and Cell Biology, Warszawa, Poland; [3]Sanquin Research, Amsterdam, The Netherlands; [4]Centre Diagnostic et Recherche CGD, TIM-C Imag, Centre National de la Recherche Scientifique (CNRS), Université Joseph Fourier, Grenoble, France; [5]Professor Hess Kinderklinik, Klinikum Bremen-Mitte, Bremen, Germany; [6]Child Health, Division of Translational Medicine, University of Manchester, Manchester, United Kingdom; [7]Allergy/Immunology Division, Children's Hospital of Michigan, Wayne State University, Detroit, Michigan; [8]GeneDx, Gaithersburg, Maryland; [9]Department of Pediatrics, American University of Beirut-Medical Center, Beirut, Lebanon; [10]Laboratory of Human Genetics of Infectious Diseases, Institut National de la Santé et de la Recherche Médicale, U550, Paris, France; [11]Paris René Descartes University, Necker Medical School, Paris, France; [12]Max-Planck-Institute for Molecular Cell Biology and Genetics, Dresden, Germany; [13]Karl Landsteiner Laboratory, Academic Medical Centre, University of Amsterdam, Amsterdam, The Netherlands; [14]Department of Biochemistry, American University of Beirut-Medical Center, Beirut, Lebanon.

Communicated by Haig H. Kazazian, Jr.

Received 28 April 2009; accepted revised manuscript 3 November 2009.
Published online 1 December 2009 in Wiley InterScience (www.interscience.wiley.com). DOI 10.1002/humu.21156

ABSTRACT: Mutations that impair expression or function of the components of the phagocyte NADPH oxidase complex cause chronic granulomatous disease (CGD), which is associated with life-threatening infections and dysregulated granulomatous inflammation. In five CGD patients from four consanguineous families of two different ethnic backgrounds, we found similar genomic homozygous deletions of 1,380 bp comprising exon 5 of *NCF2*, which could be traced to Alu-mediated recombination events. cDNA sequencing showed in-frame deletions of phase zero exon 5, which encodes one of the tandem repeat motifs in the tetratricopeptide (TPR4) domain of p67-*phox*. The resulting shortened protein (p67Δ5) had a 10-fold reduced intracellular half-life and was unable to form a functional NADPH oxidase complex. No dominant negative inhibition of oxidase activity by p67Δ5 was observed. We conclude that Alu-induced deletion of the TPR4 domain of p67-*phox* leads to loss of function and accelerated degradation of the protein, and thus represents a new mechanism causing p67-*phox*–deficient CGD.
Hum Mutat 31:151–158, 2010. © 2009 Wiley-Liss, Inc.

KEY WORDS: recombination; immunodeficiency; phagocyte; *NCF2*

Introduction

Chronic granulomatous disease (CGD) is associated with life-threatening opportunistic infections and dysregulated inflammation, often accompanied by granuloma formation even in the absence of detectable infections [Schuetz et al., 2007; Segal et al., 2000; Winkelstein et al., 2000]. Patients need regular medical checkups [Roesler et al., 2005], prophylactic and interventional antimicrobial and/or antiinflammatory treatment [Margolis et al., 1990; Mouy et al., 1994], and in certain cases bone-marrow transplantation [Schuetz et al., 2007; Seger et al., 2002]. Gene therapy may be a future therapeutic option [Ryser et al., 2007].

The phagocyte NADPH oxidase multienzyme complex is needed for appropriate microbial killing and regulation of inflammation. CGD is caused by mutations affecting the expression or function of one out of four components of this enzyme complex [van den Berg et al., 2009]. These components are gp91-*phox* (also referred to as NOX2), p22-*phox*, p47-*phox*, and p67-*phox*, (MIM#s 608515, 233710; -*phox*, *ph*agocyte *ox*idase). Rac2, p40-*phox*, and severe G6PD deficiency also cause CGD-like diseases, but are accompanied by different symptoms [Ambruso et al., 2000]. In about two-thirds of all CGD cases, mutations are found in the X-chromosomal *CYBB* gene encoding gp91-*phox*/NOX2 [Rae et al., 1998; Roesler et al., 1999]. The genetic aberrations are family-specific and comprise a wide range of mutation types. Mutations are also family-specific in p22-*phox* [Yamada et al., 2000] and—as reported so far—in p67-*phox* [Patino et al., 1999] deficiencies, which are much rarer than the X-linked form (each ~5% of all CGD cases). In contrast, p47-*phox* deficiency (~25% of all CGD cases [Roesler et al., 2000]) is mostly

[†]Marcus Gentsch, Aneta Kaczmarczyk, Dirk Roos, and Joachim Roesler contributed equally to this work.

Current address for Magdalena Kaus-Drobek: Cardiff University, Schools of Chemistry and Biosciences, Park Place, CF10 3AT Cardiff, United Kingdom.

Additional Supporting Information may be found in the online version of this article.

*Correspondence to: Joachim Roesler, MD, PhD, Dept. of Pediatrics, University Hospital Carl Gustav Carus, Fetscher Str. 74, 01307 Dresden, Germany. E-mail: Roeslerj@rcs.urz.tu-dresden.de

due to recombination events between the *NCF1* gene and one out of two highly homologous pseudogenes, thus leading to the same GT deletion at the beginning of exon 2 in ~90% of all p47-*phox*–deficient CGD patients.

In healthy individuals, the p67-*phox* protein combines with other components of the NADPH oxidase to form the fully-functional reactive oxygen species (ROS)-producing enzyme complex [Grizot et al., 2001; Mizuki et al., 2005]. The SH3 domain close to the C-terminal end of p67-*phox* interacts with the proline-rich region (PRR) of p47-*phox*, the PB1 domain links p67-*phox* to p40-*phox*, and the tetratricopeptide repeat (TPR) region of p67-*phox* domain binds Rac-GTP [Grizot et al., 2001; Lapouge et al., 2000]. The TPR domain comprises four repeats, consisting of two antiparallel α-helices. An additional third α-helix follows the fourth repeat.

A review [Deininger and Batzer, 1999] reports 33 cases of germline genetic diseases and 16 cases of cancer caused by unequal homologous recombination between Alu repeats. The authors estimate that this mode of mutagenesis accounts for 0.3% of human genetic diseases. Alu sequences are the most abundant repetitive elements in the human genome (about 1 million copies). They emerged roughly 65 million years ago and amplified throughout primate evolution by retrotransposition [Hasler and Strub, 2006]. The large number of Alu elements within the human genome provides abundant opportunities for unequal homologous recombination events. These events often occur intrachromosomally (Fig. 1A), resulting in deletion (or duplication) of exons in a gene, but they can also occur interchromosomally (Fig. 1C), causing more complex chromosomal abnormalities [Deininger and Batzer, 1999].

In five patients of unrelated families, we describe for the first time Alu-repeat-associated genomic recombinations within the *NCF2* gene that lead to the deletion of part of the TPR domain and to p67-*phox*–deficient CGD.

Materials and Methods

The patients and/or their parents consented to blood drawing and all diagnostic testing, including genetic analysis.

Cell Lines and Culture Conditions

We used a human K562 cell model of p67-*phox*–deficient CGD (K562-67def-CGD) that was engineered to contain p47-*phox* and gp91-*phox* (and that naturally expresses p22phox mRNA). Only when K562-67def-CGD cells are transduced to also produce p67-phox do these cells become capable of generating superoxide in response to phorbol 12-myristate 13-acetate (PMA) stimulation [Leto et al., 2007]. K562 cells and Epstein-Barr virus (EBV)-immortalized patient B cells were cultured in RPMI-1640 medium supplemented with 10% (v/v) fetal bovine serum (FBS), 2 mM glutamine, 100 U/mL penicillin, and 0.1 mg/mL streptomycin.

PCR and Sequencing

Genomic DNA was isolated with the QIAamp DNA Blood kit (Qiagen, Hilden, Germany). PCR reactions were performed with AmpliTaq Gold DNA Polymerase (Applied Biosystems, Warrington, UK). DNA analysis was performed with the ABI BigDye terminator-cycle-sequencing kit (Perkin Elmer, Weiterstadt, Germany) and an ABI 377 automatic sequencer (Applied Biosystems, Foster City, CA). Aberrant sequences were confirmed on both DNA strands and in a second DNA sample to avoid PCR artifacts. The ENSEMBL *NCF2* (ENSG00000116701) sequence was used.

Quantitative RT-PCR

mRNA was extracted with the Dynabeads® mRNA direct kit (Dynal, Oslo, Norway) and reverse-transcribed into cDNA with the SuperScript First-Strand Synthesis System (Invitrogen, Paisley, UK). To determine transcriptional levels of *NCF2,* quantitative RT-PCR was performed on an ABI 7000 Sequence Detection System (Applied Biosystems, Warrington, UK). The primer sequences for *NCF2* were as follows:

- forward: 5′-CCAGAAGCATTAACCGAGACAA-3′, cDNA position 182–203;
- reverse: 5′-AGAGCATCCCTCGTTGGAAGT-3′, position 221–241;
- probe: 5′-FAM-CACTTGGCAGTGGCT-TAMRA-3′, position 205–219.

Gene transcription of *NCF2* was normalized to transcription of glyceraldehyde-3-phosphate dehydrogenase (*GAPDH*) using the following primers:

- forward: 5′-GAAGGTGAAGGTCGGAGTC-3′, position 6–24;
- reverse: 5′-GAAGATGGTGATGGGATTTC-3′, position 212–231;
- probe: 5′-FAM-GGCTGAGAACGGGAAGCTTG-TAMRA-3′, position 183–202.

Retroviral Vectors and Vector Production

Full-length p67-*phox*-cDNA was ligated into *Nde*I/*Xho*I-opened pET15b (Novagen; Merck Chemicals, Darmstadt, Germany), to obtain pET15b-p67. To remove exon 5, we applied overlap extension PCR and ligated the final PCR product into *Avr*II/*Nco*I-opened pET15b-p67 to obtain pET.p67Δ5. Full-length p67-*phox* and p67-*phox*Δ5 were PCR amplified and cloned into a bicistronic gammaretroviral transfer vector [Roesler et al., 2002] (MFG-S-transgene-internal ribosome entry site [IRES]-enhanced green fluorescent protein [eGFP]). The vectors obtained, pM.p67.iG and pM.p67Δ5.iG, enable coexpression of p67-*phox* or p67Δ5 and eGFP.

Virus-particle-containing medium was from HEK 293T cells cotransfected in 10-cm dishes with 10 μg of transfer vector (pM.p67.iG or pM.p67Δ5.iG), 2 μg pMD.G (vesicular stomatitus virus glycoprotein envelope plasmid), and 6.5 μg of pHIT60 (gag-pol-packaging plasmid) in the presence of 6.75 μg/mL polyethyleneimine. K562 cells were transduced with virus-containing media in the presence of protamine sulfate (5 μg/mL) and by using spinocculation (1,200 g, 30 min). Transduction efficiency was analyzed by flow cytometry (FACS Calibur; BD Biosciences, San Jose, CA) and found to be 70% for both vectors.

Assays for NADPH Oxidase Activity

Superoxide (O_2^-) production in patients' neutrophils, EBV-B-cells, and transduced K562 cells was measured (i.e., three experiments in duplicate) by chemiluminescence over 45 min after stimulation with 1 μg/mL phorbol-12-myristate-13-acetate (PMA) in a luminol-based chemiluminescence cocktail (Diogenes; National Diagnostics, Atlanta, GA) in a Mithras LB 940 microplate reader (Berthold Technology, Bad Wildbad, Germany). Alternatively, hydrogen peroxide release by PMA-stimulated neutrophils was measured with the Amplex Red assay (Invitrogen, Carlsbad, CA) in the presence of horseradish peroxidase (HRP).

Determination of Flavocytochrome b_{558} Expression and H2O2 Production at the Single-Cell Level

The dihydrorhodamine-1,2,3 flow cytometry assay (DHR assay) for NADPH–oxidase-dependent production of ROS in neutrophils,

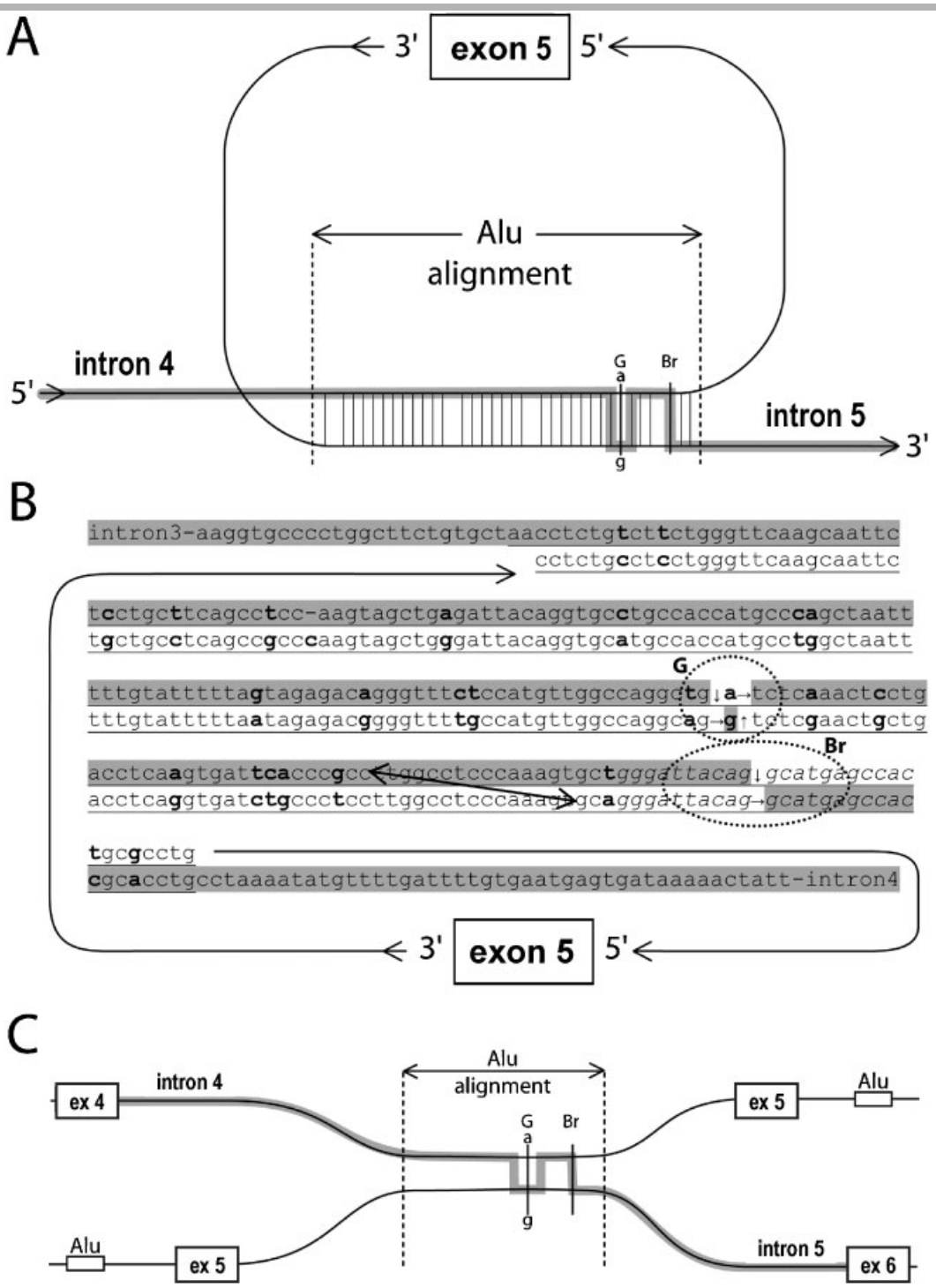

Figure 1. An AluSq-repeat upstream of exon 5 of the *NCF2* gene recombines with an AluSx-repeat downstream of exon 5, leading to a 1,380-bp deletion comprising exon 5. **A:** Schematic representation of a possible loop-forming event. **B:** The same loop and the Alu alignment in detail. The sequence that was found in all patients from Lebanon is marked in gray. All sequences not marked, whether depicted in detail or represented by a line, were found to be deleted. The Alu repeats are underlined, and mismatches between them are marked in bold. These mismatches narrow down the possible crossover point area. The main religation point (breakpoint, Br) is located within the sequence marked in italics (however, the breakpoint shown is arbitrary). The "G" marks an accompanying small gene conversion. The sequence found here had the "g" instead of the "a." The patient from Pakistan had a breakpoint slightly upstream of Br (double arrow) and no gene conversion. **C:** Instead of a recombination event within one *NCF2* allele, such an event might have happened between two different alleles (different chromosomes). Location: The *NCF2* sequence can be found on chromosome 1 at location 181,791,321–181,826,339 according to ENSEMBL. The deletion is found at approximately 181,809,587–181,810, 967 in the Lebanese families and the deletion in the patient from Pakistan is located a few bp upstream.

as indicated by H_2O_2 production, was used as described [Mauch et al., 2007]. Staining with the monoclonal antibody (moAb) 7D5, which specifically binds to an extracellular epitope of gp91-*phox*, was performed according to standard techniques. Samples were analyzed by flow cytometry (FACS Calibur; BD Biosciences, San Jose, CA).

Sample Preparation and Western Blotting

Neutrophils, K562, or EBV-B cells were washed with PBS, the pellets were solubilized in radioimmunoprecipitation assay (RIPA) buffer (Sigma-Aldrich, St. Louis, MO) with 1 mM phenylmethylsulfonyl fluoride (PMSF) and denatured at 95°C after addition of SDS sample buffer (Roti®-Load, Roth, Karlsruhe, Germany). Probes were run on 12.5% (w/v) polyacrylamide gels and transferred onto nitrocellulose membranes. After incubation with the moAb specific for p67-*phox* (1:500 diluted, catalog 610912, raised against amino acids 317–469; Becton Dickinson, Heidelberg, Germany) or for β-actin (1:5,000 diluted, clone AC-74; Sigma), respectively, and a secondary rabbit-anti-mouse-immunoglobulin (Ig) polyclonal Ab conjugated to HRP (1:2,000, P 0260; DakoCytomation, Glostrup, Denmark), the blots were developed with Amersham enhanced chemiluminescence (ECL) Plus™ Western Blotting Detection Reagents (GE Healthcare, Freiburg, Germany).

Pulse-Chase Experiments

EBV-B cells or transduced K562 cells were washed twice with warm PBS and incubated for 30 min at 5×10^6 per mL in methionine and cysteine-free RPMI 1640 medium supplemented with 2 mM L-glutamine, 1 μM L-methionine, 25 mM HEPES pH 7.5, and 10% (v/v) dialyzed FBS. For labeling, 50 μCi [^{35}S]Met-label (Hartmann Analytic GmbH, Braunschweig, Germany) were added per milliliter of Met/Cys-free medium, and the cells were incubated at 37°C for 1 hr. After labeling, the cells were washed once with PBS and chased in complete RPMI 1640 medium with 25 mM HEPES pH 7.5. Samples containing 1×10^7 B cells or 5×10^6 K562 cells were taken at indicated time points, washed twice with ice-cold PBS, and lysed in 600 μL of standard RIPA buffer containing protease inhibitor cocktail (Sigma P8340; Sigma).

Immunoprecipitation and Autoradiography

Cell lysates were precleared three times with 25 μL of protein-A agarose (Roche Applied Science, Mannheim, Germany) rotating the tubes end-over-end for 3 hr or overnight at 4°C. Subsequently, the lysates were incubated with 1 μL of the anti-p67-*phox* antiserum (Upstate, Lake Placid, NY) for 1 hr at 4°C, then 10 μL of protein A agarose were added, and the lysates were incubated for 3 hr or overnight at 4°C. The beads were washed twice with RIPA buffer and once with 10 mM Tris-HCl pH 8.0. Thereafter, beads were boiled in SDS sample buffer for 5 min and the supernatant was loaded onto 10% (w/v) polyacrylamide gels. The gels were dried and exposed to a phosphorimaging screen. Quantification was done with the ImageQuant software (Amersham Pharmacia, Uppsala, Sweden) and normalized to the initial intensity set at 100%.

Results

Identification of the p67-*phox* Deficiency

The determination of the defective disease-causing gene is exemplified in two siblings of consanguineous Lebanese parents, a boy and a girl (Patients 1 and 2, P1 and P2, respectively, in the figures) suffering from symptoms typical for CGD (Supp. Information–Case Reports). DHR testing and measurement of superoxide production of neutrophils and EBV-B cells from both patients confirmed the diagnosis of CGD without residual NADPH oxidase activity (Fig. 2A

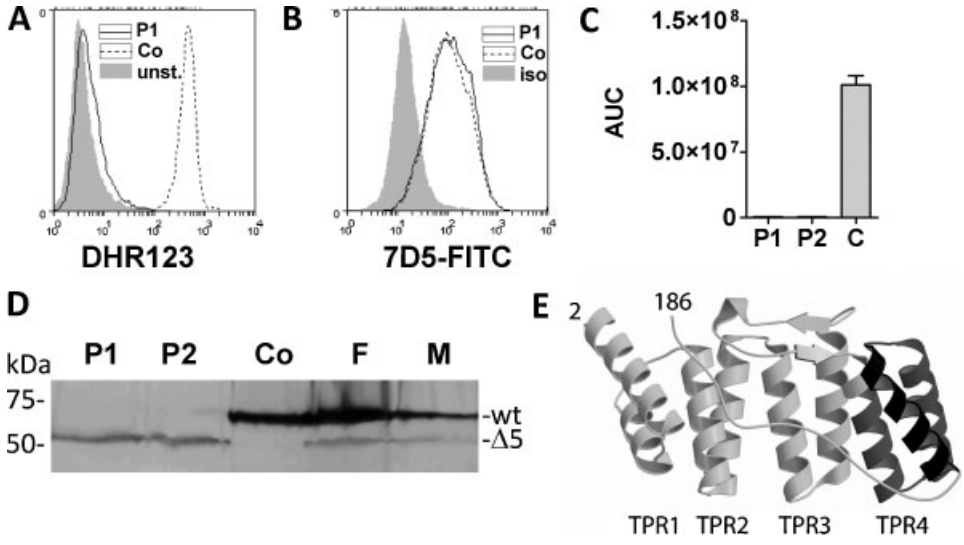

Figure 2. Deletions within the p67-*phox* protein result in failure of ROS production. **A:** PMA-stimulated granulocytes from Lebanese Patient 1 (P1; a similar result was obtained with cells from Patient 2) did not produce ROS (DHR assay); Co, healthy control donor; unst, unstimulated cells. **B:** EBV-B cells from a healthy control donor (Co) and Patient 1 (P1) were stained with 7D5 anti-gp91-*phox* antibody and analyzed by flow cytometry. Analogous data were obtained with cells from Patient 2. **C:** Failure of superoxide production by EBV-B cells from Patients 1 and 2 (P1 and P2); C, control EBV-B cells. Superoxide production was detected by a luminol-based chemiluminescence assay of PMA-stimulated cells and is given in AUC (area under the curve, arbitrary counts in 45 min). **D:** EBV-B cells from the two patients (siblings, P1 and P2), a healthy control donor (Co) and the heterozygous parents (F, father; M, mother) were analyzed for p67-*phox* expression by Western blotting with an anti-p67-*phox* monoclonal Ab (610912). Bands corresponding to the wt protein and to the mutated protein p67-*phox*-delta-exon 5 (p67Δ5, marked Δ5) are indicated (the same amount of total protein was loaded in each lane). The missing exon 5 comprises a stretch of 45 amino acids with a molecular weight of 5.3 kD, p.123-167delVLYNIAFMYAKKEEWKKAEEQLALATSMKSEPRHSKIDKAMECVW, leaving a truncated protein with a molecular weight of 61.7 kD. **E:** Ribbon model of the structure of the TPR domain of p67-*phox*. The coordinates for this figure were taken from a complex of this domain with Rac and GTP (pdb code 1e96) Reference [Lapouge et al., 2000]. The four tetratricopeptide repeats in p67-*phox* are labeled TPR1 to 4. In the p67Δ5 patients, TPR4 and the downstream helix (dark gray) are deleted.

and C). However, staining of the cells with monoclonal 7D5 antibody specific against human gp91-*phox*, followed by flow cytometry, demonstrated the presence of the membrane subunits of the enzyme (Fig. 2B) and pointed to a cytosolic factor deficiency. Since lack of p47-*phox* is usually associated with residual H_2O_2 production seen in the DHR assay, this combination of findings was highly suspicious of p67-*phox* deficiency. Indeed, by Western blotting no full-length p67-*phox* was detected in cell extracts from EBV-B cells from the two children. Instead, a faster migrating band, which was also present in EBV-B cell extracts from both parents, was recognized by the anti-p67-*phox* monoclonal antibody (Fig. 2D). This faster migrating band (referred to as Δ5 in Fig. 2D) was not seen in a sample from a patient with a complete lack of p67-*phox* (Fig. 3B) and in a control sample.

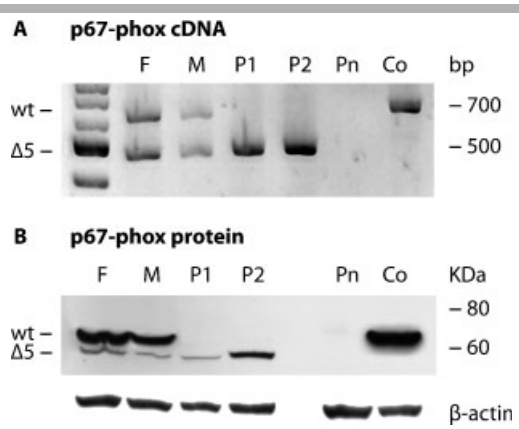

Figure 3. EBV-B cells from Patients 1 and 2 (P1 and P2) and their parents produce normal amounts of p67Δ5 mRNA, but contain low amounts of the respective p67Δ5 protein. **A:** cDNA was amplified with primers located in exons 3 and 9; 24, 26, 28, and 30 PCR cycles were applied. As shown, bands became visible after 26 cycles. The wt and the p67Δ5 (Δ5) bands were equally strong in the father (F) and in the mother (M), and the intensity of the bands was also similar in the patients (P1 and P2) compared to the control sample (Co) from a healthy donor. Negative control sample (Pn): EBV-B cells from a patient with an exon3+2T>C mutation and thus without exon 3 and without p67-*phox* expression. **B:** Western blot of EBV-B cells from the same patients with the anti-p67-phox (610912) and the β-actin (AC-74) monoclonal Ab, respectively. (The variation in intensity of the Δ5 band between F, M, P1, and P2 cannot be explained completely. However, the Western blot has been repeated at least five times. The variation was much less pronounced in the first two experiments (Fig. 2D), but increased after the EBV-B cells had been cultured for a longer period. Therefore, the variation in Δ5 band intensity is most probably a matter of EBV-B cell subclone formation, meaning that the fastest growing subclones express the Δ5 protein differently.

Moreover, the Δ5 band was much fainter than that of wild-type (wt) p67-*phox*. This was also the case in the parents and thus in cell extracts that contained both p67-*phox* protein forms (Figs. 2D and 3B), indicating decreased synthesis or enhanced degradation of the protein or its mRNA.

Sequencing of the p67-*phox* (*NCF2*) cDNA from the patients revealed that exon 5 of p67-*phox* was missing without a frameshift or any additional sequence changes. The consanguineous parents were both heterozygous for the deletion (Fig. 3A), and their neutrophils produced normal amounts of ROS (data not shown).

In the other three families, the consanguineous parents were from Lebanon or Pakistan. No normal or faster migrating p67-*phox* bands were identified in Western blot analysis of EBV-B cells or neutrophil from the patients in these families (Table 1).

Alu Element Recombination Causes the Exon 5 Deletion in *NCF2*

We suspected a splice mutation adjacent to or at the 5′ or 3′ end of exon 5 in the *NCF2* gene. Instead, PCR reactions with diverse primers located upstream and downstream of this exon gave no amplification product, indicating a large deletion. In a next step, roughly 400-bp-long, overlapping stretches of DNA of introns 4 and 5 were amplified to find the approximate localization of the deletion. Then, a PCR reaction was performed with a pair of primers located within the amplimers that could be obtained upstream and downstream adjacent to the deletion. The PCR product was sequenced to identify the religation point (breakpoint or crossover point; Fig. 1).

The identified sequence is marked in gray in Figure 1. This mutation (c.366+2401_502-527del1380, p.V123_W167del) had not been described before. Comparison with the standard ENSEMBL sequence revealed the localization of the religation point within an Alu repeat that had recombined from two separate Alu repeats, one upstream and one downstream of exon 5. The location of this crossover point could be estimated thanks to the mismatches in the Alu repeats (Figure 1B, marked in bold). In 5′ to 3′ direction, the sequence found in the patients first followed the AluSq repeat [Price et al., 2004] upstream of exon 5. At the crossover point, it changed to the AluSx repeat downstream of exon 5. Interestingly, there is one exception to this general rule: in the site marked G in Fig. 1, the guanine nucleotide of AluSx is found instead of the adenine of AluSq, demonstrating a small gene conversion.

Table 1. Summary of Results Obtained From the Patients*

	Consanguineous families			
	Family 1 (Patients 1 and 2)	Family 2 (Patient 3)	Family 3 (Patient 4)	Family 4 (Patient 5)
Ethnic background	Lebanese	Lebanese	Lebanese	Pakistani
NADPH oxidase activity in neutrophils	Nil	Nil	Nil	Nil
P67-*phox* expression in neutrophils	NT	Nil	NT	NT
P67-*phox* expression in EBV-B cells	Low amount p67Δ5	Nil or trace[a]	NT	NT
Crossover point in AluSq/Sx-hybrid Alu-repeat	←----------between-8T/C and –30T/A----------→ (Fig. 2B; Br)			Between –30T/A and –50G/T (Fig. 2B; ↔)
Gene conversion –82A>G in AluSq as part of recombined Alu (Fig. 2B and G)	Yes	Yes	Yes	No

The bp numbering refers to the hybrid AluSq/Sx-repeat sequence, arbitrarily counting backward from the 3′ to the 5′ end with the last bp as –1 (Fig. 1B).
[a]The discrepancy with Family 1 could be due to differences in blotting techniques or to an even faster degradation of p67Δ5 in cells from Patient 3 than in cells from Patients 1 and 2 (compare to Fig. 4). NT, not tested.

The sequences of all patients from Lebanon were all identical to those marked in gray in Figure 1B, including the small gene conversion, whereas the crossover point was slightly more upstream in the patient from Pakistan (Fig. 1B, double arrow), and no gene conversion was observed. In agreement with these observations, a 1,380-bp deletion comprising exon 5 was found in all five patients. The findings are summarized in Table 1.

Stability of p67Δ5 mRNA and Protein

Next, we evaluated possible explanations for the low amount of p67Δ5 protein in the patients' cells, as exemplified in one of the Lebanese families (Fig. 3B). The difference in band intensity was not caused by different binding of the p67-*phox* monoclonal Ab, since equal amounts of recombinant p67-*phox* and p67-*phox*Δ5 gave similarly strong bands (Supp. Fig. S1). Moreover, the epitope against which the antibody was raised lies outside the exon-5-encoded region (epitope amino acids 317–469, deletion amino acids 123–167).

We detected equal amounts of p67-*phox* and p67-*phox*Δ5 mRNA by gel electrophoresis of low-cycle-number RT-PCR products (Fig. 3A) and by quantitative RT-PCR (Table 2). Pulse-chase experiments with EBV-B cells from the mother started out with equal amounts of the full-length and the truncated p67-*phox* protein (Fig. 4B, right side). This demonstrates that up to the point of protein synthesis there was no quantitative difference between the two forms. However, once synthesized, the fate of the two forms differed. The truncated form was degraded more rapidly (Fig. 4). Transduced K562 cells also showed a vastly decreased half-life of the p67Δ5 variant in comparison to the full-length protein (Fig. 4, left side). This suggests that the p67Δ5 protein was misfolded and hence quickly degraded.

Table 2. TaqMan RT-PCR of mRNA From EBV-Transformed B-Cells*

	Cycle threshold GAPDH	Cycle threshold p67 (NCF2 cDNA)
Patient 1, p67Δ5	18 ± 1	28 ± 1
Patient 2, p67Δ5	18 ± 1	28 ± 1
P67-*phox*, full-length	17 ± 1	27 ± 1

*Equal mRNA expression of both the mutated (Patients 1 and 2) and the wild-type (control) p67-*phox* ($n = 2$, cycle threshold ± range).

Influence of p67Δ5 on ROS Production

The deletion of exon 5 leads to a deletion of 45 amino acids without frameshift or amino acid change at the exon borders. In the wt protein the deleted fragment would fold into the three alpha helices of the TPR4 region (Fig. 2E).

The TPR domain of p67-*phox* is responsible for the binding of Rac-GTP, which is needed for activation of the NADPH-oxidase complex. The residues that interact with Rac-GTP are located in the loops connecting TPR1 to TPR2 (S37) and TPR2 to TPR3 (D67 and H69), and in the inserted β-hairpin between TPR3 and TPR4 (R102, N104, L106, and D108) [Lapouge et al., 2000]. Hence, the TPR4 subdomain and the α-helix adjacent downstream of TPR4 that are missing from p67Δ5 are not directly involved in Rac-GTP binding (Fig. 2E). Therefore, we hypothesized that p67-*phox*Δ5 might have residual NADPH-oxidase-activating functionality but cannot be detected due to the fast degradation of this protein.

To test this hypothesis we used CGD model K562 cells that permanently express all components of the NADPH oxidase with the exception of p67-*phox*, and transduced these cells with retroviral vectors expressing either p67-*phox*Δ5 or wt p67-*phox* in the first cistron and EGFP in the second cistron. Transduction efficiency was determined by flow cytometry and found to be 70% for both vectors (Supp. Fig. S2). Western blot analyses showed

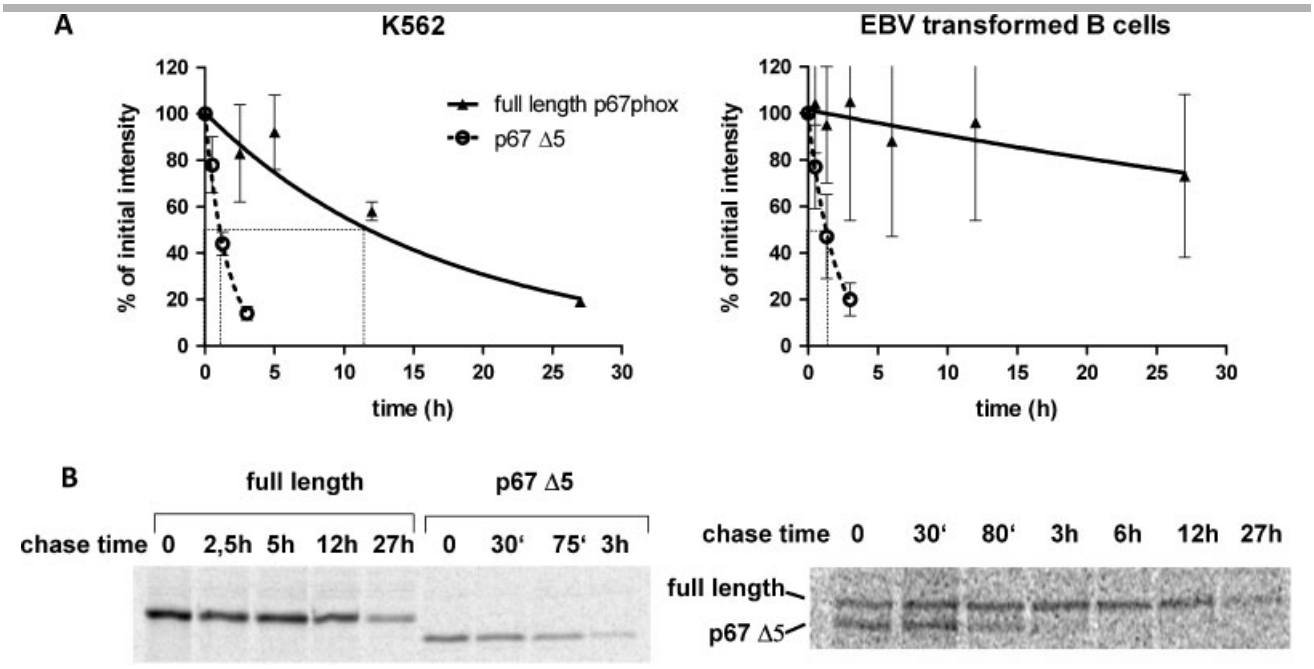

Figure 4. The half-life of p67Δ5 is approximately 10-fold shorter than that of the wt p67-*phox*. K562 cells transduced with cDNA encoding either full-length p67-*phox* or mutated p67Δ5 and EBV-B cells from the Lebanese mother of Patients 1 and 2 (P1 and P2) were labeled with [^{35}S]methionine for 1 hr and chased for the times indicated. The cell lysates were analyzed by immunoprecipitation with p67-*phox* antiserum, followed by SDS-PAGE and phosphorimaging. **A:** Band intensities of at least three independent experiments were quantified and plotted against the chase times (mean values ± SD). **B:** Representative autoradiographs.

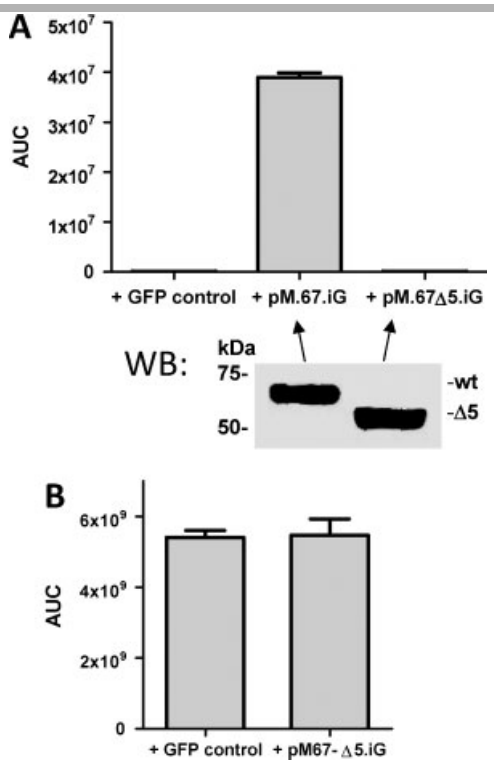

Figure 5. The mutated p67-*phox* protein (p67Δ5) cannot interact to form a functional NADPH oxidase and has no dominant negative effect. **A:** Production of ROS was measured by chemiluminescence (AUC: area under the curve of arbitrary counts in 45 min) after PMA activation of K562 cells that permanently express all components of the NADPH oxidase except p67-*phox*. These cells were transduced with a GFP control vector, with wild-type p67-*phox* (pM.67.iG) or with p67Δ5 (pM.67Δ5.iG). Western blot analysis (WB) reveals strong expression of p67-*phox* and of p67Δ5 (the same amount of total protein was loaded in each lane). Effective transduction has also been ensured by flow cytometric determination of GFP expression from the second cistron (Supp. Fig. S2). **B:** ROS production by K562 cells that already permanently expressed all components of the NADPH oxidase and that were additionally transduced either with a GFP control vector or with pM.67Δ5.iG.

equally strong expression of wt p67-*phox* and p67Δ5. However, also with these cells, no detectable ROS production was found in cells expressing p67-*phox*Δ5 (Fig. 5A). On the other hand, ROS production by activated K562 cells that contain all components of the NADPH oxidase including p67-*phox* was not functionally inhibited by additional transduction with p67Δ5 (Fig. 5B). These results indicate that p67Δ5 does not significantly interfere with NADPH oxidase assembly.

Taken together, the p67-*phox*Δ5 protein is nonfunctional, does not interfere with normal NADPH oxidase assembly if wt p67-*phox* is present (it has no dominant negative effect), and is rapidly degraded.

Discussion

Our patients suffered from classical symptoms of CGD, and p67-*phox* deficiency was detected as the underlying reason. In all five patients, an Alu-repeat-induced 1,380-bp deletion comprising exon 5 of the *NCF2* gene resulted in the deletion of 45 amino acids from p67-*phox*, forming the TPR4 sequence and the downstream helix. The results of the transduction and p67Δ5 pulse-chase experiments suggest misfolding and accelerated degradation of p67Δ5.

The Alu-repeat induced sequence variation of the Pakistani family differed from that of the three Lebanese families. The latter families were not directly related and lived in different countries in Europe and the United States. Nevertheless, a founder effect is the most likely reason why they had exactly the same sequence variation. However, such an effect does not provide a general explanation for all four families. Rather, the propensity of Alu-repeats to recombine must be the reason for all deletions found. This is the first report demonstrating that such recombination accounts for a fraction of p67-*phox*–deficient CGD cases.

A number of germline genetic diseases and types of cancer are caused by unequal homologous recombination between Alu-repeats. Alu-repeat-mediated interaction between the *NCF1* gene and its pseudogenes has been discussed as a possible reason for such recombination events in p47-*phox*–deficient CGD [Roesler et al., 2000]. In addition, a deletion in the *NCF1* gene (c.154-285_451+821del2860, p.Lys52ThrfsX82) has been found to be flanked by Alu sequences. Furthermore, Alu repeats may be implicated in large chromosomal deletions involving the *CYBB* gene, but they have never been directly shown to be involved in CGD [Brown et al., 1996]. However, it has been clearly demonstrated that several cases of other diseases, such as hemophilia [Nakaya et al., 2004], pseudoxanthoma elasticum [Katona et al., 2005], and familial and sporadic paraganglioma [Baysal et al., 2004], are caused by homologous recombination between Alu sequences, mostly leading to deletions. Alu sequences have also been described to modulate gene expression at the posttranscriptional level. Furthermore, Alu sequences may contribute to evolution by providing crossover points for genetic recombination and gene duplication and have been used to trace primate evolution [Salem et al., 2003].

As in other diseases resulting from Alu-induced deletions (e.g., Rossetti et al. [2004]), we found an additional small gene conversion close to the breakpoint. This may be explained as follows: the recombination process probably starts with the formation of a stretch of heteroduplex DNA before DNA sense and antisense strands are disrupted and are religated crosswise. The mismatches in the heteroduplex DNA (Fig. 1B) may then be removed by DNA repair enzymes that use one strand as a template to which they adapt the other strand. For some reason, the strand used as a template and the strand adapted to it may sometimes change. This may also apply to the region where the crossover point was found, and therefore the real site(s) where DNA has been physically cut off may be at some distance from the point indicated (Fig. 1B).

In most other cases of p67-*phox*–deficient CGD characterized so far, no p67-*phox* protein was detected in patient cells [Noack et al., 1999]. Only a few mutations, such as the deletion of Lys-58, permit production of an apparently stable protein. However, this ΔK58 variant was unable to bind Rac-GTP and to translocate to the membrane [Leusen et al., 1996]. For the amino-acid substitutions and small in-frame deletions described by others [Noack et al., 1999; Patino et al., 1999], the lack or diminished levels of the protein may be a consequence of structural instability and increased susceptibility to intracellular proteases, similar to the case described in our work.

Taken together, p67-*phox*–deficient CGD adds to the diseases that can be caused by Alu-repeat-induced genomic deletions. Our results also indicate that the TPR4 domain of p67-*phox* is necessary for proper protein folding, stability and, thus, function.

Acknowledgments

We thank Alexander Herr, Department of Human Genetics, for interesting discussions and helpful search of the literature; Claudia Stihlo, Department

of Immunology, MTZ, for anti-p67-*phox*-antibodies; Katrin Höhne, University Children's Hospital, for excellent assistance; Frank Pessler, University Children's Hospital, for critical reading of the manuscript and helpful comments; Andrea Gross (Center for Graphic Design, MRZ), for expert graphic design (University Hospital, Technical University of Dresden, Dresden, Germany), and Tom Leto, National Institutes of Health (NIH), National Institute of Allergy and Infectious Diseases (NIAID), Bethesda, MD, for kindly providing CGD model K562 cells.

References

Ambruso DR, Knall C, Abell AN, Panepinto J, Kurkchubasche A, Thurman G, Gonzalez-Aller C, Hiester A, deBoer M, Harbeck RJ, Oyer R, Johnson GL, Roos D. 2000. Human neutrophil immunodeficiency syndrome is associated with an inhibitory Rac2 mutation. Proc Natl Acad Sci USA 97:4654–4659.

Baysal BE, Willett-Brozick JE, Filho PA, Lawrence EC, Myers EN, Ferrell RE. 2004. An Alu-mediated partial SDHC deletion causes familial and sporadic paraganglioma. J Med Genet 41:703–709.

Brown J, Dry KL, Edgar AJ, Pryde FE, Hardwick LJ, Aldred MA, Lester DH, Boyle S, Kaplan J, Dufier JL, Ho MF, Monaco AM, Musarella MA, Wright AF. 1996. Analysis of three deletion breakpoints in Xp21.1 and the further localization of RP3. Genomics 37:200–210.

Deininger PL, Batzer MA. 1999. Alu repeats and human disease. Mol Genet Metab 67:183–193.

Grizot S, Fieschi F, Dagher MC, Pebay-Peyroula E. 2001. The active N-terminal region of p67phox. Structure at 1.8 A resolution and biochemical characterizations of the A128V mutant implicated in chronic granulomatous disease. J Biol Chem 276:21627–21631.

Hasler J, Strub K. 2006. Alu elements as regulators of gene expression. Nucleic Acids Res 34:5491–5497.

Katona E, Aslanidis C, Remenyik E, Csikos M, Karpati S, Paragh G, Schmitz G. 2005. Identification of a novel deletion in the ABCC6 gene leading to pseudoxanthoma elasticum. J Dermatol Sci 40:115–121.

Lapouge K, Smith SJ, Walker PA, Gamblin SJ, Smerdon SJ, Rittinger K. 2000. Structure of the TPR domain of p67phox in complex with Rac.GTP. Mol Cell 6:899–907.

Leto TL, Lavigne MC, Homoyounpour N, Lekstrom K, Linton G, Malech HL, de Mendez I. 2007. The K-562 cell model for analysis of neutrophil NADPH oxidase function. Methods Mol Biol 412:365–383.

Leusen JH, de KA, Hilarius PM, Ahlin A, Palmblad J, Smith CI, Diekmann D, Hall A, Verhoeven AJ, Roos D. 1996. Disturbed interaction of p21-rac with mutated p67-phox causes chronic granulomatous disease. J Exp Med 184: 1243–1249.

Margolis DM, Melnick DA, Alling DW, Gallin JI. 1990. Trimethoprim-sulfamethoxazole prophylaxis in the management of chronic granulomatous disease. J Infect Dis 162:723–726.

Mauch L, Lun A, O'Gorman MR, Harris JS, Schulze I, Zychlinsky A, Fuchs T, Oelschlagel U, Brenner S, Kutter D, Rosen-Wolff A, Roesler J. 2007. Chronic granulomatous disease (CGD) and complete myeloperoxidase deficiency both yield strongly reduced dihydrorhodamine 123 test signals but can be easily discerned in routine testing for CGD. Clin Chem 53:890–896.

Mizuki K, Takeya R, Kuribayashi F, Nobuhisa I, Kohda D, Nunoi H, Takeshige K, Sumimoto H. 2005. A region C-terminal to the proline-rich core of p47phox regulates activation of the phagocyte NADPH oxidase by interacting with the C-terminal SH3 domain of p67phox. Arch Biochem Biophys 444: 185–194.

Mouy R, Veber F, Blanche S, Donadieu J, Brauner R, Levron JC, Griscelli C, Fischer A. 1994. Long-term itraconazole prophylaxis against Aspergillus infections in thirty-two patients with chronic granulomatous disease. J Pediatr 125:998–1003.

Nakaya SM, Hsu TC, Geraghty SJ, Manco-Johnson MJ, Thompson AR. 2004. Severe hemophilia A due to a 1.3 kb factor VIII gene deletion including exon 24: homologous recombination between 41 bp within an Alu repeat sequence in introns 23 and 24. J Thromb Haemost 2:1941–1945.

Noack D, Rae J, Cross AR, Munoz J, Salmen S, Mendoza JA, Rossi N, Curnutte JT, Heyworth PG. 1999. Autosomal recessive chronic granulomatous disease caused by novel mutations in NCF-2, the gene encoding the p67-phox component of phagocyte NADPH oxidase. Hum Genet 105:460–467.

Patino PJ, Rae J, Noack D, Erickson R, Ding J, de Olarte DG, Curnutte JT. 1999. Molecular characterization of autosomal recessive chronic granulomatous disease caused by a defect of the nicotinamide adenine dinucleotide phosphate (reduced form) oxidase component p67-phox. Blood 94:2505–2514.

Price AL, Eskin E, Pevzner PA. 2004. Whole-genome analysis of Alu repeat elements reveals complex evolutionary history. Genome Res 14:2245–2252.

Rae J, Newburger PE, Dinauer MC, Noack D, Hopkins PJ, Kuruto R, Curnutte JT. 1998. X-Linked chronic granulomatous disease: mutations in the CYBB gene encoding the gp91-phox component of respiratory-burst oxidase. Am J Hum Genet 62:1320–1331.

Roesler J, Heyden S, Burdelski M, Schafer H, Kreth HW, Lehmann R, Paul D, Marzahn J, Gahr M, Rosen-Wolff A. 1999. Uncommon missense and splice mutations and resulting biochemical phenotypes in German patients with X-linked chronic granulomatous disease. Exp Hematol 27:505–511.

Roesler J, Curnutte JT, Rae J, Barrett D, Patino P, Chanock SJ, Goerlach A. 2000. Recombination events between the p47-phox gene and its highly homologous pseudogenes are the main cause of autosomal recessive chronic granulomatous disease. Blood 95:2150–2156.

Roesler J, Brenner S, Bukovsky AA, Whiting-Theobald N, Dull T, Kelly M, Civin CI, Malech HL. 2002. Third-generation, self-inactivating gp91(phox) lentivector corrects the oxidase defect in NOD/SCID mouse-repopulating peripheral blood-mobilized CD34+ cells from patients with X-linked chronic granulomatous disease. Blood 100:4381–4390.

Roesler J, Koch A, Porksen G, von BH, Brenner S, Hahn G, Fischer R, Lorenz N, Gahr M, Rosen-Wolff A. 2005. Benefit assessment of preventive medical check-ups in patients suffering from chronic granulomatous disease (CGD). J Eval Clin Pract 11: 513–521.

Rossetti LC, Goodeve A, Larripa IB, De Brasi CD. 2004. Homeologous recombination between AluSx-sequences as a cause of hemophilia. Hum Mutat 24:440.

Ryser MF, Roesler J, Gentsch M, Brenner S. 2007. Gene therapy for chronic granulomatous disease. Expert Opin Biol Ther 7:1799–1809.

Salem AH, Ray DA, Xing J, Callinan PA, Myers JS, Hedges DJ, Garber RK, Witherspoon DJ, Jorde LB, Batzer MA. 2003. Alu elements and hominid phylogenetics. Proc Natl Acad Sci USA 100:12787–12791.

Schuetz C, Hoenig M, Schulz A, Lee-Kirsch MA, Roesler J, Friedrich W, von Bernuth H. 2007. Successful unrelated bone marrow transplantation in a child with chronic granulomatous disease complicated by pulmonary and cerebral granuloma formation. Eur J Pediatr 166:785–788.

Segal BH, Leto TL, Gallin JI, Malech HL, Holland SM. 2000. Genetic, biochemical, and clinical features of chronic granulomatous disease. Medicine (Baltimore) 79:170–200.

Seger RA, Gungor T, Belohradsky BH, Blanche S, Bordigoni P, Di Bartolomeo P, Flood T, Landais P, Müller S, Ozsahin H, Passwell JH, Porta F, Slavin S, Wulffraat N, Zintl F, Nagler A, Cant A, Fischer A. 2002. Treatment of chronic granulomatous disease with myeloablative conditioning and an unmodified hemopoietic allograft: a survey of the European experience, 1985–2000. Blood 100:4344–4350.

van den Berg JM, van Koppen E, Ahlin A, Belohradsky BH, Bernatowska E, Corbeel L, Español T, Fischer A, Kurenko-Deptuch M, Mouy R, Petropoulou T, Roesler J, Seger R, Stasia MJ, Valerius NH, Weening RS, Wolach B, Roos D, Kuijpers TW. 2009. Chronic granulomatous disease: the European experience. PLoS One 4:e5234.

Winkelstein JA, Marino MC, Johnston Jr RB, Boyle J, Curnutte J, Gallin JI, Malech HL, Holland SM, Ochs H, Quie P, Buckley RH, Foster CB, Chanock SJ, Dickler H. 2000. Chronic granulomatous disease. Report on a national registry of 368 patients. Medicine (Baltimore) 79:155–169.

Yamada M, Ariga T, Kawamura N, Ohtsu M, Imajoh-Ohmi S, Ohshika E, Tatsuzawa O, Kobayashi K, Sakiyama Y. 2000. Genetic studies of three Japanese patients with p22-phox-deficient chronic granulomatous disease: detection of a possible common mutant CYBA allele in Japan and a genotype-phenotype correlation in these patients. Br J Haematol 108:511–517.